Chromium enriched peraluminous glasses: solubility limits, crystalline phase equilibrium and impact of chromium on the rheological properties of the glass

Erik Hansen, Damien Perret, Isabelle Giboire, Sylvain Mure, Pierre-Jean Panteix, Christophe Rapin

Chromium enriched peraluminous glasses: solubility limits, crystalline phase equilibrium and impact of chromium on the rheological properties of the glass

E. Hansen [a], D. Perret [a], I. Bardez-Giboire [a], S. Mure [a], P.J. Panteix [b], C. Rapin [b]

[a] *CEA, DES, ISEC, DE2D, SEVT, Laboratoire d'études de Développement des Matrices de Conditionnement, Univ Montpellier, Marcoule, France*

[b] *Institut Jean Lamour, Nancy, France*

* Corresponding author.
Email address: damien.perret@cea.fr
Full postal address: CEA, DES, ISEC, DE2D, Univ Montpellier, Centre de Marcoule, BP 17171, 30207 Bagnols-sur-Cèze cedex

ABSTRACT

Chromium is a multivalent element with very low solubility in silica-based glasses. It is incorporated into glass via the solubilisation of Cr_2O_3 as Cr^{3+} through an acido-basic reaction, and is in redox equilibrium with Cr^{6+} and Cr^{2+} oxidation states depending on the surrounding atmosphere. The least soluble form of chromium is Cr^{3+}, which is also the most common form of chromium in glass elaborated in air. This study investigated the behaviour of chromium in peraluminous glasses, which are potential matrices for nuclear waste containment. Chromium is often present in nuclear waste solutions as a corrosion product coming from the waste reprocessing steps. Consequently, it is important to understand the effect of chromium addition to peraluminous glasses, both in terms of the microstructure and the processing ability of the glass melt. The study investigated the effect of chromium added as a Cr_2O_3 chromium (+III) oxide on the homogeneity, the viscosity, and the glass transition temperature (T_g) of peraluminous glasses. The chromium redox state and its effect on the incorporation limit of chromium was determined. Peraluminous glasses have an incorporation limit of between 0.50 and 0.55 wt. % Cr_2O_3 in air, and between 1.25 and 1.50 wt. % Cr_2O_3 in a reducing environment. Chromium (+III) oxide was found to have a limited effect on the viscosity of peraluminous glasses up to 2 wt.% of Cr_2O_3, despite the presence of crystals above 0.5 wt. %. The addition of chromium oxide had no significant effect on the T_g of the glass, except after a slow cooling of the sample containing the highest content of 2.0 wt. % Cr_2O_3 Two forms of chromium were identified under UV-visible spectroscopy for the glasses elaborated in air: Cr^{3+} (6-fold) and Cr^{6+} (4-fold).

Keywords:

Peraluminous glass, Nuclear waste glass, Incorporation limit, Redox, Viscosity, Chromium

1. Introduction

Chromium is often added to glass as a nucleating agent to form glass-ceramics [1]. This is mainly due to the very low incorporation limit of Cr^{3+} in most glasses [2-3]. It may also be introduced as a colouring agent, as Cr^{3+} gives a bright green colouring at low content, Cr^{2+} a light blue colour, and Cr^{6+} a yellow colour [4]. It may also be present in nuclear glasses when stainless steel corrosion occurs in reprocessing facilities [5-6], or in situations where chromium is added for a specific purpose, for example as a stabilizing agent for a UO_2 fuel microstructure [7]. Glass crystallization cannot be allowed in certain types of nuclear glass, when the presence of crystals exposed to irradiation could damage the containment matrix properties. It is therefore important to investigate chromium

incorporation in glass, since its low solubility in that medium is a constraint limiting the nuclear waste incorporation rate, and thereby increasing the final number of waste canisters produced.

The effect of chromium addition on the physical properties of glass is not well documented. However, the impact of chromium on glass crystallization has been described [5, 8-11], as well as its speciation in glass and glass ceramics [2, 4, 12-16].

It has been demonstrated that peraluminous glasses have a high incorporation rate for rare earth elements, making them interesting candidates for the containment of nuclear waste [17-18]. Rare earth elements are present in the waste and are also used as surrogates for actinides in non-radioactive glasses. Typically, peraluminous glasses have larger amounts of alumina than of modifier oxides like alkaline oxides and alkaline earth oxides. The parameter describing the peraluminous nature of the glass is called the Rp ratio:

$$Rp = \frac{modifiers}{Al2O3+modifiers} \qquad (1)$$

An Rp ratio lower than 0.5 means a deficit in modifiers to compensate for the negative charge of aluminium as a network intermediate, and makes the glass a peraluminous glass. An Rp ratio higher than 0.5 makes the glass a peralkaline glass. Since the behaviour of chromium in peraluminous glass is almost unknown, this work first focused on determining the incorporation limit of chromium (+III) oxide Cr_2O_3 in peraluminous glasses, taking into account thermal history of the glass. The valence and coordination of chromium were studied, as chromium solubility was expected to be strongly dependant on its valence. The effect of chromium on the viscosity and glass transition temperature were also investigated. Finally, the impact of the oxygen partial pressure on chromium solubility in peraluminous glass was evaluated through comparative measurements performed in air atmosphere and in a reducing environment.

2. Experimental

2.1. Glass elaboration

An optimized composition for peraluminous glass taken from Piovesan et al. [18] was used as a reference for this work, as this composition has demonstrated potential interest for nuclear waste conditioning. From the initial composition, re-named EH BASE 0, glass compositions were designed with a Cr_2O_3 content increasing from 0.25 wt. % to 2.00 wt. % (Table 1).

Table 1: Glass compositions (wt. %)

Glass wt %	**EH BASE-0**	**EH Cr-0.25**	**EH Cr-0.5**	**EH Cr-0.55**	**EH Cr-0.6**	**EH Cr-0.75**	**EH Cr-1**	**EH Cr-1.5**	**EH Cr-2**
SiO_2	30.96	30.89	30.81	30.79	30.78	30.73	30.65	30.50	30.35
CaO	2.95	2.94	2.94	2.93	2.93	2.93	2.92	2.91	2.89
Li_2O	0.59	0.59	0.59	0.59	0.59	0.59	0.58	0.58	0.58
La_2O_3	26.11	26.05	25.98	25.97	25.96	25.92	25.85	25.72	25.59
Al_2O_3	20.44	20.39	20.33	20.32	20.31	20.28	20.23	20.13	20.03
B_2O_3	16.11	16.07	16.03	16.02	16.01	15.99	15.95	15.87	15.76
Na_2O	2.84	2.83	2.83	2.82	2.82	2.82	2.81	2.80	2.78
Cr_2O_3	**0.00**	**0.25**	**0.50**	**0.55**	**0.60**	**0.75**	**1.00**	**1.50**	**2.00**
Total	100.00	100.00	100.00	100.00	100.00	100.00	100.00	100.00	100.00

Nine 200g glass batches were prepared at 1350° in a muffle furnace. The glass samples were obtained from two preparation paths, either after a fast cooling rate (as-quenched samples), or after a slow cooling rate (slowly cooled samples). As-quenched glasses can be considered to be representative

of the steel-glass interfacial layer of a nuclear waste canister, while slowly cooled glasses are more representative of the canister core. The experimental procedure for glass sample elaboration has been described by Hansen et al. [19]. The mixture of oxide precursors included SiO_2, CaO, Li_2CO_3, La_2O_3, Al_2O_3, H_3BO_3, Na_2CO_3, and Cr_2O_3 powders from Sigma Aldrich. The corresponding precursor purities are 0.994, 0.999, 0.990, 1.000, 1.000, 0.999, 1.000, and 0.990, respectively. The experimental error for the weighing was ±0.002 g. The batches were preheated in Pt-Rh alloy crucibles for decarbonisation at 500°C for 3h, followed by melting at 1350°C for 3h. Due to the highly refractory nature of peraluminous glasses and chromium oxide, a double fusion process was used to avoid unmelted particles. The resulting glasses were cast onto a stainless steel plate before being crushed. They were then milled down into powder in a tungsten carbide (WC) mill with WC marbles (300t/min, 3x2min). Following this step, the glasses were melted again at 1350°C for 2h. The samples obtained after quenching were the as-quenched glasses (AQ). Approximately 40g of these as-quenched glasses were re-melted for 45 minutes at 1350°C in a Pt-Au crucible before being slowly cooled at 1°C/minute until room temperature was reached. The glasses obtained from this second treatment were the slowly cooled glasses (SC).

Reduced glasses with controlled oxygen partial pressure were prepared in fused silica tubes containing the glass and a Fe/FeO redox buffer. This buffer ensues an oxygen partial pressure of 10^{-10} atm at 1350°C [20]. 100 mg glass beads were initially shaped by melting them in graphite crucibles. To ensure that the beads were representative of the bulk glasses, preliminary tests were carried out at 1350°C in the silica tubes in order to determine the amount of time needed to replicate the bulk state. The use of small sized beads enabled a fast equilibration with the surrounding atmosphere and a constant Surface/Volume ratio, ensuring reproducible experiments. The silica tubes containing the glass beads and the buffer were sealed and heated for 5h at 1350°C, before air quenching. The device is shown in Figure 1.

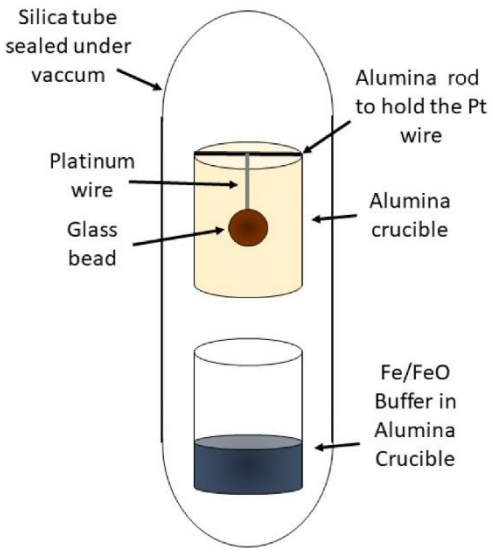

Figure 1: Experimental setup for glass elaboration under controlled oxygen partial pressure, reproduced from [20]

The amorphous or partially crystallized natures of the samples were investigated using optical microscopy, Scanning Electron Microscopy (SEM), and X-Ray Diffraction (XRD) analyses. The

crystalline phase composition was determined by comparing EDS (Energy Dispersive X-Ray Spectroscopy) measurements and XRD results.

2.2. Glass characterization

The XRD spectra were measured with a conventional Bragg-Brentano diffractometer (Paralytical X'Pert MPD Pro – Cu anti cathode). The samples were crushed into a powder finer than 100 microns in a WC mill, and placed into stainless steel holders. The data collection range was 2Θ = 10-90°. The XRD peaks were compared to crystalline phases detailed in the Joint Committee on Powder Diffraction Standards (JCPDS) PDF4+ database, using the 5.0 version of the EVA software.

Optical microscopy was carried out with a ZEISS Axio Imager.M2 microscope. It was connected to an Axiocam 305 camera and EC Epiplan-Neofluar x1.25, x5, x20, x50 and x100 HD DIC M27 lenses. The samples had been polished to mirror quality. Images were taken and analysed with the Zen2Core v2.5 software.

Scanning Electron Microscopy (SEM ZEISS SUPRA 55, 15 kV) and EDS analysis were performed on polished, carbon covered (in a 10 nm layer) samples. Significant amounts of data on crystalline phase composition were collected through EDS measurements which, in combination with XRD patterns, allowed hypotheses to be made regarding the composition of the crystalline phases present. Data collection and processing were carried out using the ESPRIT 2.0 software.

UV-Visible spectra were obtained using a CARY50SCAN spectrophotometer, with a wavelength range of 200-1100 nm. The CARY WINUV software was used for the data processing, and the UV-Visible spectra were deconvoluted using the OriginPro2015 software. Due to the high absorbance of Cr^{6+} in this wavelength range, thin lamella samples were made (thickness about 100µm).

Viscosity measurements were performed using a LAMY RM300i imposed-stress rheometer. The rheometer was placed on top of a vertical tubular furnace, with a functioning range of 1000-1500°C. The glass samples were first melted at 1200°C in Pt-Rh crucibles (crucible radius R_e = 13.5 mm). Then each crucible was placed in the centre of the furnace. The temperature gradient measured from top to bottom of the sample was lower than 2°C. A Pt cylinder suspended from the rheometer was immersed and rotated in the melt. Rheological measurements were carried out in a steady state regime by imposing successive shear stress values, ranging from 1 to 500 Pa, for 60s. Angular velocity measurements were averaged when the signal was stationary, i.e. during the last 10s. The rheological behaviour was measured for temperatures ranging from 1050°C to 1500°C. The relative standard error on viscosity measurements was estimated to be ±10%, based on historical data obtained for the setup.

Glass transition temperatures (Tg) were extrapolated from Differential Thermal Analysis (DTA). About 50g of glass powder were heated in alumina crucibles. A SETSYS Evolution DTA furnace from SETARAM was used to make the DTA measurements, and the associated software was SETSYS-1750Cs Evol.-TG-DTA 1600°C. The Tg was obtained from the DTA data using SETARAM CALISTO Processing software. The standard error on Tg was estimated to be ± 6°C.

3. Results

3.1. Incorporation limits of chromium in glasses elaborated in air

The incorporation limits for Cr_2O_3 in peraluminous glasses were determined taking into account the thermal history of the glass. The incorporation limits were thus determined for both as-quenched glasses cast at 1350°C, and glasses slowly cooled at 1°C/minute. The incorporation limits of Cr_2O_3 for both thermal scenario were determined to be between 0.50 wt % and 0.55 wt %.

3.2. Crystallization behaviour of glasses elaborated in air

The crystalline phases observed in both as-quenched and slowly cooled glass samples appeared for the same amounts of Cr_2O_3, and had similar morphologies and compositions. The principal crystalline phase had a layered shape, with a pure Cr_2O_3 core and a surrounding layer of $Cr_{2-x}Al_xO_3$ (with $0 < x < 0.6$).

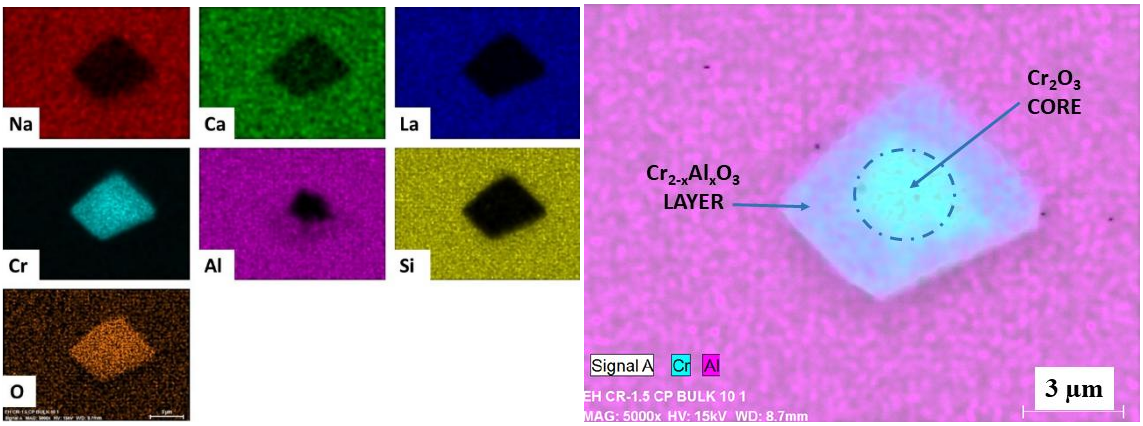

Figure 2: Crystal cartography in EH Cr-1.5 as-quenched sample, showing a Cr_2O_3 core and a $Cr_{2-x}Al_xO_3$ outer layer

The XRD diffractograms were peak-matched to the $Cr_{1.28}Al_{0.72}O_3$ phase detailed in the JCPDS card n°04-007-6151 (Figure 11, in Appendix), which had also been studied and elaborated using different techniques by Zhang et al. [21]. The pure Cr_2O_3 phase was not detected under XRD analysis.

3.3. UV-Visible study of chromium valence and coordination

UV-Visible spectroscopy identified two valences for the glasses elaborated in air: Cr^{3+} and Cr^{6+} (

Figure 3). The absorption spectra were very similar for both as-quenched and slowly cooled glasses, showing the same transitions. The spectra were deconvoluted using Gaussian curves to fit with the respective contributions of Cr^{3+} and Cr^{6+}. The evolutions of these contributions with increasing Cr_2O_3 contents are shown in Figure 4. The molar extinction coefficients of Cr^{6+} and Cr^{3+} are widely different, and therefore comparisons of peak areas can only be qualitative. They may however highlight certain trends. The relative contribution of Cr^{6+} was stronger in slowly cooled glasses than in as-quenched glasses (70% and 50%, respectively). Additionally, the contributions of the Cr^{6+} and Cr^{3+} valence and coordination appear to be dependant on the Cr_2O_3 content. From the peak positions on the deconvoluted curves and data from the literature [22-26], Cr^{3+} was identified as having a 6-fold coordination and Cr^{6+} as having a 4-fold coordination. Two peaks were identified for Cr^{3+}, around 420nm and 630nm, corresponding respectively to the $^4A_2 \rightarrow {}^4T_1(F)$ and $^4A_2 \rightarrow {}^4T_2(F)$ transitions. The

characteristic very intense peak of Cr^{6+} was identified at around 360nm, and corresponds to the $^4A_{2g} \rightarrow {}^4A_{1g}$ transition.

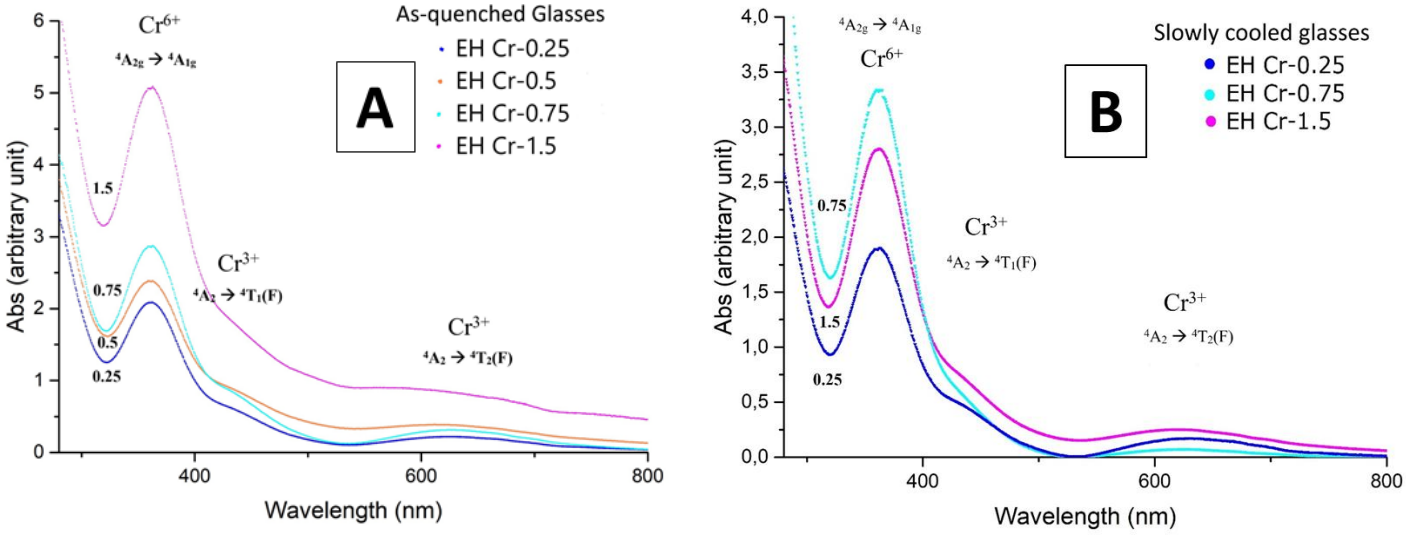

Figure 3: UV-visible spectra of (A) as-quenched glasses and (B) slowly cooled glass samples

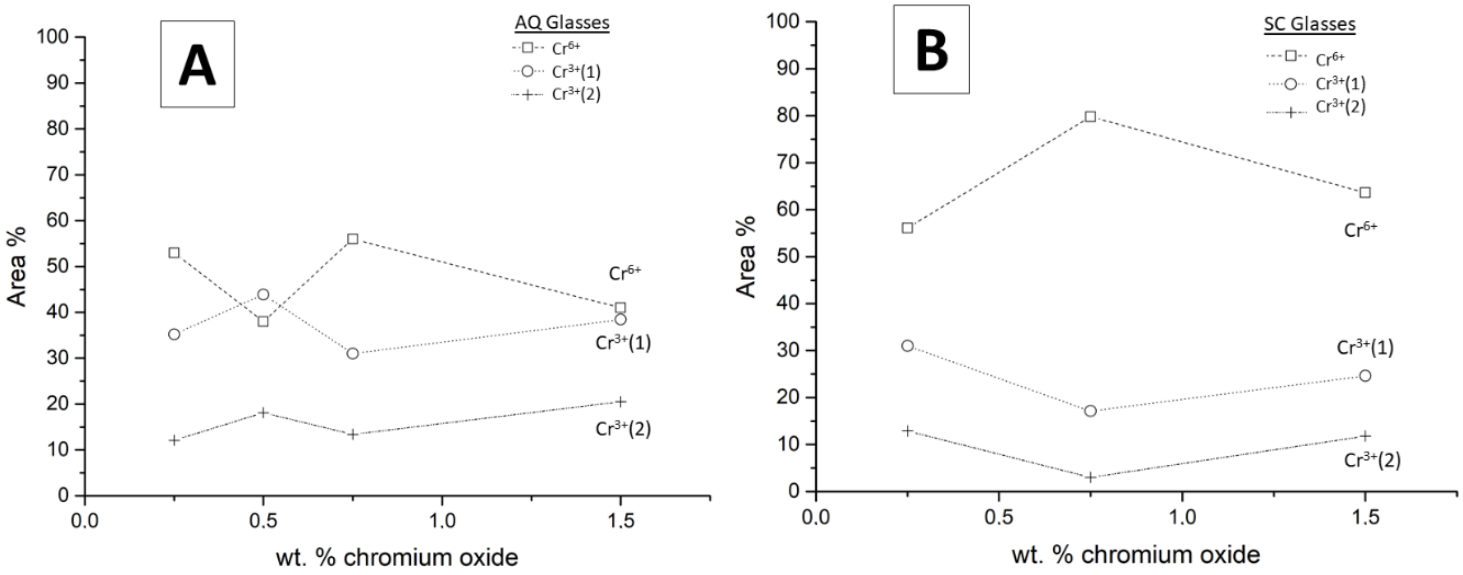

Figure 4: Evolution of the contribution of the several forms of chromium in (A) as-quenched, and (B) slowly cooled glass samples – dotted lines have been added as visual guidelines

3.4. Glass transition temperature

The glass transition temperatures (Tg) of the peraluminous glass samples were measured as a function of Cr_2O_3 content and taking into account the thermal history of the glass (Figure 5). It was found that Cr_2O_3 addition left the T_g unchanged at around 655°C, taking into account the possible experimental error. For the slowly cooled glass samples, a slight decrease of T_g (~20°C) was observed for the glass containing 2.0 wt. % of Cr_2O_3.

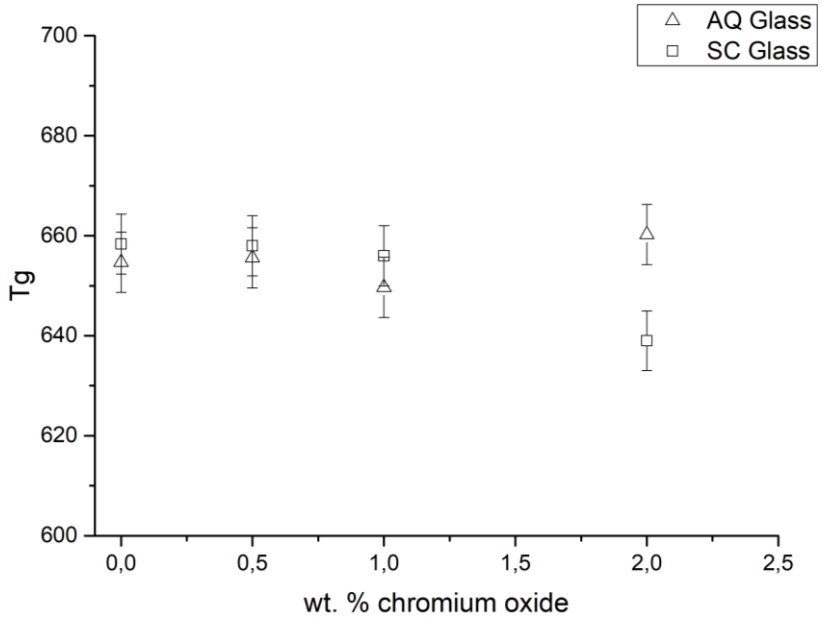

Figure 5: Glass transition temperature evolution with Cr_2O_3 content for as-quenched (AQ) and slowly cooled (SC) samples

3.5. Rheological properties

The addition of chromium oxide up to 2.0 wt. % Cr_2O_3 in the peraluminous glass left the viscosity almost unchanged, when experimental error was taken into account (Figure 6). This remained true despite the presence of crystals above 0.5 wt. % Cr_2O_3. Nevertheless, there was a slight tendency for the viscosity to decrease with a Cr_2O_3 content below 0.50 wt. %, followed by an increase when the Cr_2O_3 content was between 0.50 and 1.00 wt.%, and then a very slight decrease between 1.00 and 2.00 wt. % Cr_2O_3. Again, this may not be meaningful, due to experimental error. However the trend might be related to the behaviour of the melt and the presence of crystals, as detailed in the Discussion section below.

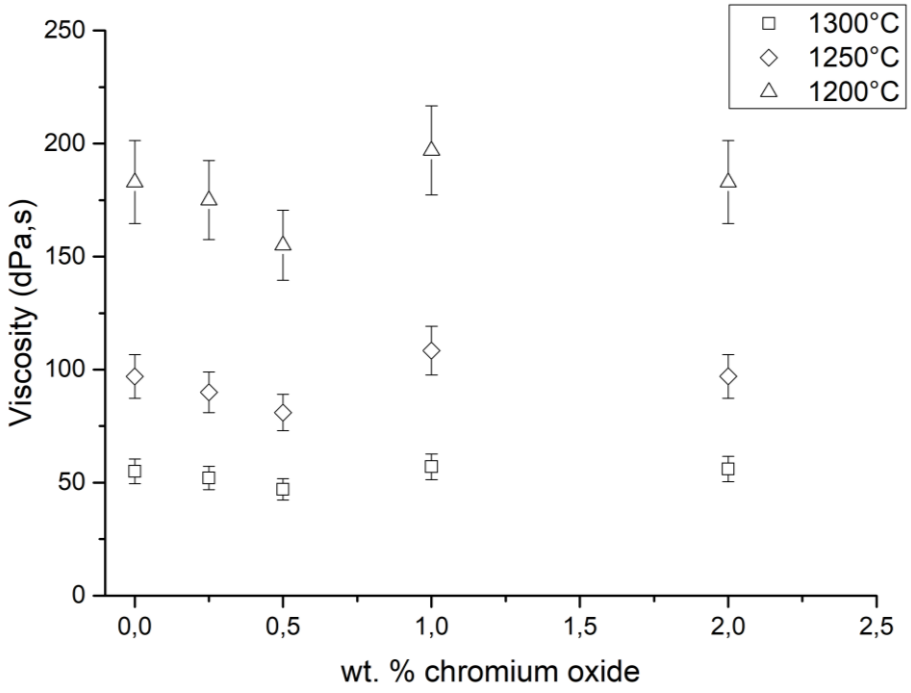

Figure 6: Glass melt viscosity evolution with Cr_2O_3 content

3.6. Influence of the oxygen partial pressure

In silicate glasses, the least soluble form of chromium is known to be Cr^{3+}, whereas Cr^{6+} and Cr^{2+} are more soluble in a glass melt [2]. Cr^{6+} is the other predominant form of chromium for oxidizing atmospheres, whilst Cr^{2+} can be present only under very reducing conditions. In order to determine the influence of a reducing environment on the solubility of chromium in peraluminous glasses at 1350°C, glass beads were made with a chromium (+III) oxide content beyond its incorporation limit as determined under air, i.e. under an oxygen partial pressure of 0.2 atmosphere. Glass beads containing 0.75, 1.00, 1.25, and 1.50 wt. % Cr_2O_3 were made under reducing conditions using a Fe/FeO buffer as described before, providing an oxygen partial pressure of 10^{-10} atm.

Among the beads made under reducing conditions, the beads containing 0.75, 1.00, and 1.25 wt.% Cr_2O_3 were homogeneous and fully amorphous, while the bead containing 1.50 wt.% Cr_2O_3 presented crystalline phases. The results are given in Table 2. The incorporation limit of chromium oxide in peraluminous glass under reduced conditions is therefore between 1.25 and 1.50 wt. %.

Table 2: Crystallized (C) or homogeneous (H) nature of the glass beads with respect to Cr_2O_3 content and oxygen partial pressure (pO_2)

wt. % Cr_2O_3	0.75	1.00	1.25	1.50
pO_2 = 0.2 atm	C	C	C	C
$pO_2 = 10^{-10}$ atm	H	H	H	C

Cr-, Al-, and O-rich crystals could be seen in the glass containing 1.50 wt. % Cr_2O_3 elaborated in a reducing environment. Their compositions are given in Table 3. XRD could not be carried out on this glass, as the sample amount was too small. Based on our previous observations of similar crystals in

glass elaborated in air, we made the assumption that these were $Cr_{2-x}Al_xO_3$ crystals. Several crystal shapes were observed, including rectangles and straw-like dendrites, as seen in Figure 7. No pure Cr_2O_3 cores were found in the crystals.

Table 3: SEM/EDS analyses of several crystals in the glass containing 1.50 wt.% Cr_2O_3 made under reducing conditions ($pO_2=10^{-10}$ atm)

	Cr (mol %)	Al (mol %)	O (mol %)
Crystals with high Al content	27.4	12.6	60
Crystals with low Al content	31.6	8.4	60
Average	28.6	11.4	60
Equivalent $Cr_{2-x}Al_xO_3$ stoichiometry	$Cr_{1.43}Al_{0.57}O_3$		

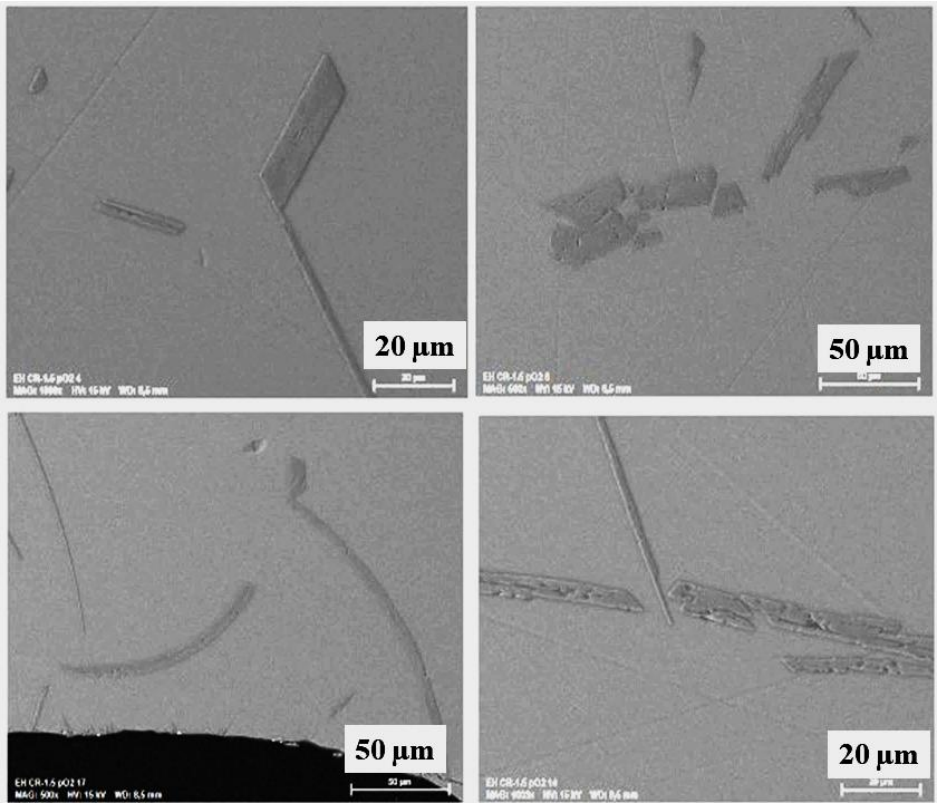

Figure 7: Several $Cr_{2-x}Al_xO_3$ crystal shapes in the EH Cr-1.5 reduced glass

4. Discussion

The solubilisation of Cr_2O_3 in the glass melt initially occurs based on the acido-basic reaction:

$$Cr_2O_3 = 2Cr^{(III)}O_x^{(2x-3)-} + (3-2x)\ O^{2-} \quad (2)$$

The Cr^{3+} formed is in redox equilibrium with the other oxidation states, Cr^{2+} and Cr^{6+}. The Cr^{3+}, the most prevalent form of chromium in glasses elaborated in air, is the least soluble of the oxidized forms

of Cr. Because of this low solubility, only a few mass percent of chromium were added to the glass composition for this study. Hence, the intrinsic properties of the glass were not greatly modified.

4.1. Chromium incorporation limit

The incorporation limit of chromium in peraluminous glass elaborated at 1350°C in air was determined to be between 0.50 and 0.55 wt. % Cr_2O_3. As a comparison, the incorporation limits of other corrosion elements such as Fe and Ni in similar glasses are much higher, and show significant differences between as-quenched and slowly cooled glasses [19, 27].

This incorporation limit of chromium under reducing conditions was determined to be between 1.25 and 1.50 wt.% Cr_2O_3, significantly higher than the limit in glasses elaborated in air. Under reducing conditions, chromium was present under its +II valence which is known to be much more soluble than the Cr^{3+} valency [2].

When the chromium incorporation limit was exceeded, glasses elaborated under both conditions, i.e. in air or under a reducing atmosphere, formed the same kind of crystalline phase, $Cr_{2-x}Al_xO_3$ (Figure 2).

For the glasses elaborated in air, the stoichiometry of this phase was matched to $Cr_{1.28}Al_{0.72}O_3$ from XRD analysis (Figure 11 in appendix). This composition evolved from the centre of the crystal to its periphery, with the amount of Al gradually increasing (Figure 10 Table 6 in appendix). These chromia-like crystals were very small in size, never exceeding 10 microns, and very numerous. The fact that crystals were present at 0.55 wt. % Cr_2O_3 in both as-quenched and slowly cooled glasses lead to inferring that the crystalline phase was already present in the glass melt at high temperature. This is also in accordance with the high liquidus temperatures of chromium oxide containing crystals [5]. A slight difference in morphology could be observed between the crystalline phases in as-quenched and slowly cooled samples, typically in the global size of the crystals and in the Cr_2O_3 core size. A Cr_2O_3 nucleus could serve as a site for nucleation, from which the crystalline growth would incorporate aluminium from the surrounding glass.

Under reducing conditions, the Cr^{2+} valence did not appear in the final crystals, as the only phase observed was a chromia-type phase made of Cr^{3+}. The crystals were rather massive compared to those present in the glasses elaborated in air. They also had different shapes and did not have the layer/core dual composition. They could span over 25 microns as rectangles, and over more than 100 microns as straw-like crystals. Even though what could cause such a difference in morphology is uncertain, the main changing parameter was that the crystallizing Cr^{3+} was no longer mainly in equilibrium with Cr^{6+}, but would be in equilibrium with Cr^{2+}. The fact that Cr^{2+} did not appear in the final crystals does not mean that it was not involved in the crystallization process. A two-step mechanism involving both $Cr^{2+}$and Cr^{3+} species has already been described in the literature [2]:

(i) acido-basic reaction of Cr_2O_3 dissolution into Cr^{3+} species
and
(ii) reduction of Cr^{3+} into Cr^{2+}

$Cr_{2-x}Al_xO_3$ crystal growth is determined by the availability of both chromium cations (i.e. Cr^{2+}, Cr^{3+}, and Cr^{6+}) and Al^{3+} in its vicinity. It has been shown that the Cr^{2+} diffusion coefficient in glass is two to three orders of magnitude higher than that of Cr^{6+}, and is comparable to that of Cr^{3+} as reported by Schmucker et al. [28]. Furthermore, crystal enlargement under reduced conditions can be fostered by the atomic transport of Cr^{2+} in the vicinity of Cr_2O_3 crystals, which are then oxidized into Cr^{3+} and inserted into Cr_2O_3. Conversely, the lower diffusion of Cr^{6+} in glasses elaborated under air could contribute to smaller crystal sizes. A schematic view of the process is given in Figure 8.

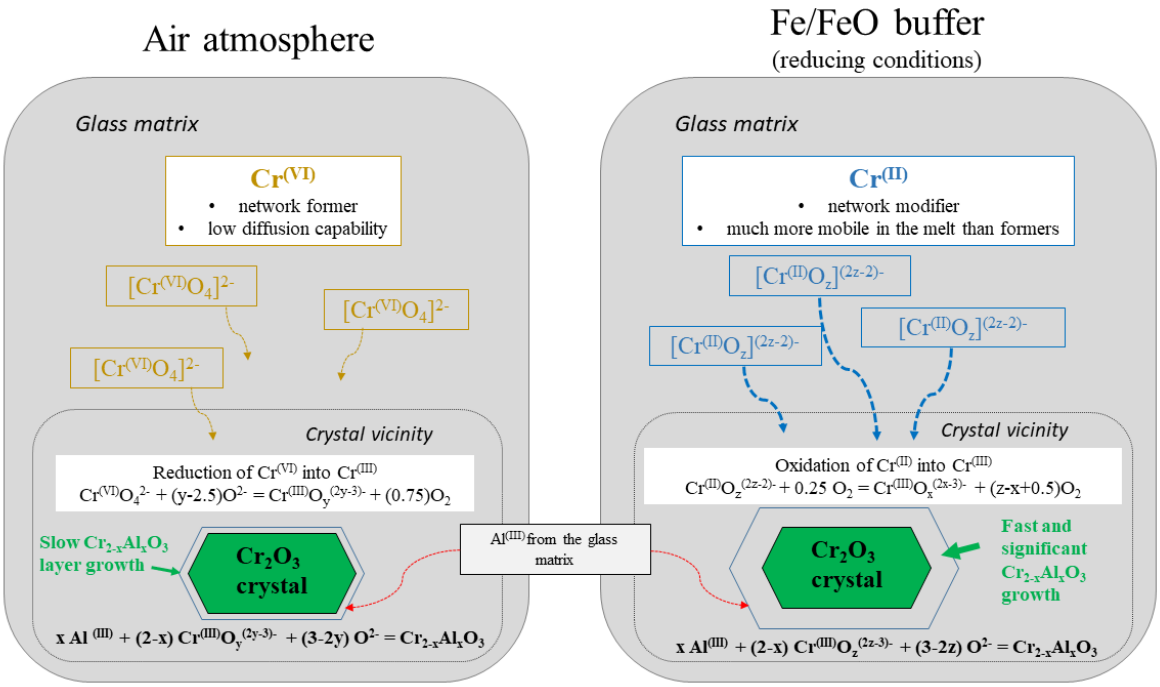

Figure 8: Difference in the hypothetical growth mechanisms in glasses elaborated in air and under reducing conditions (equations taken from [2])

4.2. Glass structure and physical properties

The glass structure was investigated through UV-Visible spectroscopy to better understand the chromium impact on the glass physical properties. UV-Visible spectroscopy could be carried out on the glass samples elaborated in air but not under reducing conditions, as the glass beads were too small to be shaped into lamella.

Cr^{3+} was identified in a 6-fold coordination with peaks located around 420nm and 630nm. Cr^{6+} was identified in a 4-fold coordination with a typical intense band around 360nm (

Figure 3). Cr^{3+} is hence expected to play a network modifier role [23-25, 29] and Cr^{6+} is expected to be present as CrO_4^{2-} tetrahedrons, acting more as a network former [24, 29].

It appears from the results that the as-quenched glasses had higher amounts of Cr^{3+} compared to the slowly cooled glasses, which is consistent with the stabilization at higher temperature of the quenched glasses favouring the reduced forms of Cr (here Cr^{3+} in equilibrium with Cr^{6+}). In slowly cooled glass, the kinetics allowed a re-oxidization of the Cr^{3+} into Cr^{6+}.

The Cr^{6+}/Cr_{tot} ratio decreased with the addition of Cr_2O_3 in the as-quenched glasses before crystallization occurred (

Figure 3). The hypothesis of an influence of the basicity on the Cr^{6+}/Cr_{tot} ratio was discarded, as the variation of the glass basicity with the addition of chromium was negligible (Table 7 and Table 8 in Appendix). The hypothesis of a competition between the CrO_4^{2-} form of Cr^{6+} and the AlO_4^- form of Al^{3+} for charge compensators (Li^+, Na^+, Ca^{2+}, La^{3+}), which would lead to a destabilisation of Cr^{6+} and the formation of Cr^{3+}, was also discarded given the calculation of the charge balance in the glass. At 0.75 wt. % Cr_2O_3, i.e. beyond the incorporation limit, the Cr^{6+}/Cr_{tot} ratio increased (Figure 4). From 0.75 to 1.5 wt.% Cr_2O_3, the Cr^{6+}/Cr_{tot} ratio in the glass once again decreased. These results could be

discarded as being artefacts related to the deconvolution process. However this trend was observed for both as-quenched and slowly cooled glasses. These variations of the Cr^{6+}/Cr_{ToT} ratio are difficult to understand but could to be correlated to the slight variation in the glass viscosity with the addition of Cr_2O_3, as explained hereafter.

The main aim of the viscosity measurements was to evaluate the influence of chromium oxide and crystals on the rheological behaviour of the glasses. Two aspects were considered:

(i) The variation of the viscosity with the addition of chromium oxide, due to glass structure modification and the apparition of crystals.
(ii) The modification of the glass rheological behaviour due to the presence of crystals in the melt, leading to a potential loss of Newtonian behaviour.

As reported in Figure 6, Cr_2O_3 addition up to 2 wt. % did not lead to significant variations in viscosity when the experimental error was taken into account. For these small amounts of Cr_2O_3 added to the glass, the viscosity variation was moderate, but the slope was not negligible. At 1250°C, the slopes were 32 dPa.s per wt.% between 0 and 0.5 wt. % Cr_2O_3, and 54 dPa.s per wt. % between 0.5 and 1.0 wt. % Cr_2O_3. As a comparison, the slopes obtained by Hansen et al. [19] for NiO addition to the same peraluminous glass were 19 dPa.s per wt.% between 0 and 1.0 wt. % NiO, and 7 dPa.s per wt.% between 1.0 and 6.5 wt. % NiO. Nevertheless, NiO was identified as having a fluidifying effect because of the large amounts (up to 15 wt. %) that could be added.

The following hypotheses have been made regarding the role of chromium on peraluminous glass viscosity:

- Cr^{6+} plays the role of a weak network former, which is in accordance with the Cr-O bond energy around 429±29 kJ/mol [33] (compared to 800 kJ/mol for Si-O and 502 kJ/mol for Al-O [34]
- Cr^{3+} plays the role of a network modifier, according to the literature [23-25, 29]. The modifier Cr^{3+} should lead to a stronger decrease in viscosity than Cr^{6+}.

From 0 to 0.5 wt. % Cr_2O_3, the dissolution of Cr_2O_3 into Cr^{3+} and Cr^{6+} lead to a decrease in viscosity. This decrease in viscosity is coherent with the network modifier role expected for Cr^{3+} and also for the weak network former role that Cr^{6+} should play, according to UV-visible spectroscopy (
Figure 3).

Above 0.5 wt. %, a viscosity increase took place that is related to the crystallization of Cr_2O_3 above its solubility limit.

Above 1 wt. %, the viscosity very slightly decreased again, despite the fact that chromium was no longer incorporated into the glass matrix. This reveals that the crystallization of the $Cr_{2-x}Al_xO_3$ phase did not lead to major modifications in the rheological behaviour of the glass. This slight viscosity decrease could be explained by the increase of Cr^{3+} as observed (Figure 9), or (less likely) by the extraction of aluminium from the matrix to the crystalline phase $Cr_{2-x}Al_xO_3$.

Lastly, it appears that even for glasses containing up to 2 wt. % Cr_2O_3, i.e. far above the incorporation limit, the amounts of crystals were too small to lead to a loss of Newtonian behaviour in the range of temperature studied (1500-1050°C). This might be linked to their shape and size distribution, as they did not form macroscopic aggregates from the microscopic crystals. This would have lead to a strong modification in the rheological behaviour. A change in the workability of the melt due to crystallization is to be avoided for any possible evolution of the nuclear waste vitrification process that might allow crystallization to occur.

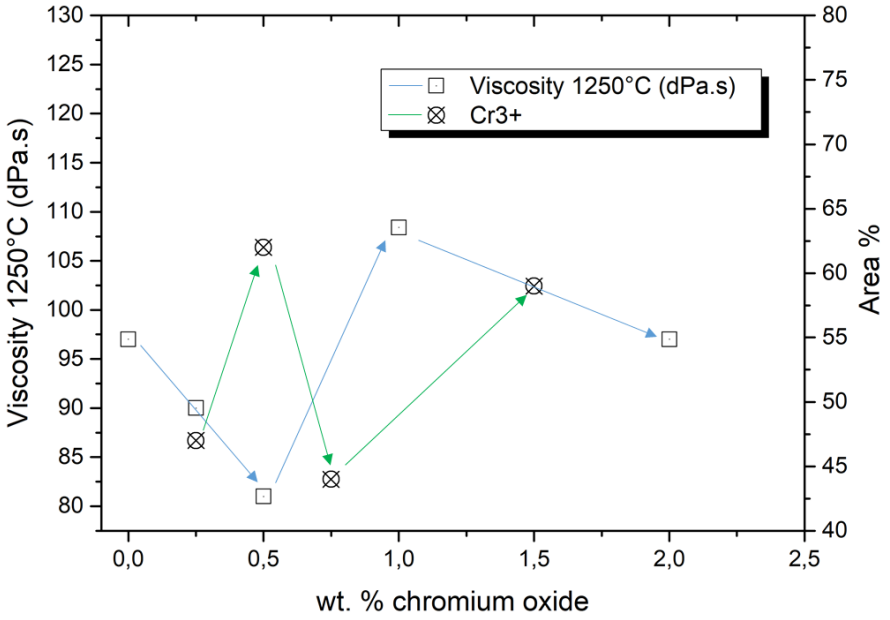

Figure 9: Comparative evolution of viscosity at 1250°C and Cr^{3+} with respect to the Cr_2O_3 content. Arrows have been added as visual guidelines

This is further supported by the DTA measurements (Figure 5). They reveal that the addition of chromium oxide only lead to a drop in the glass transition temperature (T_g) for the slowly cooled glass containing 2 wt. % of Cr_2O_3. For other glasses, the T_g seemed to remain stable, given the measurement uncertainty. This discrepancy might be caused by the fact that, because of chromium oxide crystallization, aluminium was extracted from the glass matrix to form $Cr_{2-x}Al_xO_3$. This was especially the case for the slowly cooled and Cr-rich glass. Hence aluminium, which is an element that increases the T_g, was extracted from the glass matrix, and the T_g of the residual glass was lowered.

Despite this small variation, the glass transition temperature T_g remained high enough to represent a nuclear waste reprocessing context, and met the requirement for sustaining high temperatures induced in glass from the energy released by radioactive decay.

5. Conclusions

As already observed in peralkaline silica glass compositions, chromium (+III) oxide has a very low incorporation limit in peraluminous glasses, even at high temperatures. Both quenched and slowly cooled glasses have an incorporation limit between 0.50 and 0.55 wt. % Cr_2O_3. Above the incorporation limit, chromia-like crystals were observed, with a pure chromia core and an aluminium-enriched layer. This crystalline phase remained dispersed with very small crystallites (below 10 microns). The addition of chromium oxide up to 2.0 wt. % only had a slight influence on the glass viscosity within the range studied, with no major influence on the rheological behaviour or on the glass transition temperature. Chromium was found to be in Cr^{3+}(6-fold) and Cr^{6+}(4-fold) forms in the glasses elaborated in air. An increase of the incorporation limit up to 1.25 wt. % without crystallization has been demonstrated in glasses elaborated under reducing conditions in oxygen partial pressure around 10^{-10} atm, confirming the high solubility of Cr^{2+} compared to Cr^{3+}.

6. Acknowledgement

The authors would like to thank their Orano and EDF partners for financial support.

7. References

[1] M. Rezvani, B. Eftekhari-Yekta et al. Effect of Cr_2O_3. Fe_2O_3 and TiO_2 nucleants on the crystallization behaviour of SiO_2-Al_2O_3-CaO-MgO(R_2O) glass-ceramics, Ceramics International vol. 31(1) (2005) 75-80. https://doi.org/10.1016/j.ceramint.2004.03.037

[2] H. Khedim, R. Podor, C. Rapin, M. Vilasi, Redox-Control Solubility of Chromium Oxide in Soda-silicate Melts, Journal of the American Ceramic Society 91 [11] (2008) 3571-3579. https://doi.org/10.1111/j.1551-2916.2008.02692.x

[3] J.L. Manfredo, R.N. McNally, Solubility of refractory oxides in Soda-Lime Glass, Communications of the American Ceramic Society 67 [8] (1984) C155-C158. https://doi.org/10.1111/j.1151-2916.1984.tb19178.x

[4] O. Villain, G. Calas et al. XANES determination of chromium oxidation states in glasses: Comparison with optical absorption spectroscopy, Journal of the American Ceramic Society 90(11) (2007) 3578-3581. https://doi.org/10.1111/j.1551-2916.2007.01905.x

[5] J. D. Vienna et al. Chromium phase behaviour in a multi-component borosilicate glass melt, Journal of Non-Crystalline Solids 352 (2006) 2114-2122. https://doi.org/10.1016/j.jnoncrysol.2006.02.051

[6] Monographie DEN CEA, Le conditionnement des déchets nucléaires (2008), 27.

[7] L. Barbieri, C. Leonelli et al. Solubility, reactivity and nucleation effect of Cr_2O_3 in the CaO-MgO-Al_2O_3-SiO_2 glassy system, Journal of Materials Science 29 (1994) 6273-6280. https://doi.org/10.1007/BF00354571

[8] S. Zhang, Y. Zhang, Z. Qu, Effect of soluble Cr_2O_3 on the silicate network, crystallization kinetics, mineral phase, microstructure of CaO-MgO-SiO_2-(Na_2O) glass ceramics with different CaO/MgO ratios, Ceramics International 45 (2019) 11216–11225. https://doi.org/10.1016/j.ceramint.2019.02.106

[9] B. Mirhadi, B. Mehdikhani, Crystallization behavior and microstructure of ($CaO{\cdot}ZrO_2{\cdot}SiO_2$)–$Cr_2O_3$ based glasses, Journal of Non-Crystalline Solids 357 (2011) 3711–3716. https://doi.org/10.1016/j.jnoncrysol.2011.07.040

[10] M. Mika, M.J. Schweiger, J.D. Vienna, P. Hrma, Liquidus temperature of spinel precipitating high-level waste glasses. Scientific Basis for Nuclear Waste Management XX, Materials Research Society (1997) Pittsburgh, PA, 7. https://doi.org/10.1557/PROC-465-71

[11] A.J. Berry, H. S. C. O'Neill et al. The effect of composition on Cr^{2+}/Cr^{3+} in silicate melts. American Mineralogist 91 (2006) 1901-1908. https://doi.org/10.2138/am.2006.2097

[12] V. Felice, B. Dussardier et al. Chromium-doped silica optical fibres: influence of the core composition on the Cr oxidation states and crystal field, Optical Materials 16 (2001) 269-277. https://doi.org/10.1016/S0925-3467(00)00087-2

[13] X. Feng, S. Tanabe, Spectroscopy and crystal-field analysis for Cr(IV) in aluminosilicate glasses. Optical Materials 20(1) (2002) 63-72. https://doi.org/10.1016/S0925-3467(02)00048-4

[14] N. Iwamoto and Y. Makino, State of the chromium ion in soda silicate glasses under various oxygen pressures, Journal of Non-Crystalline Solids 41(2) (1980) 257-266. https://doi.org/10.1016/0022-3093(80)90171-4

[15] Abdullah et al, Dissolution equilibrium of chromium oxide in a soda lime silicate melt exposed to oxidizing and reducing atmospheres, Materials Chemistry and Physics 142 [2-3] (2013) 572-579. https://doi.org/10.1016/j.matchemphys.2013.07.055

[16] C. Riglet-Martial, P. Martin, D. Testemale, C. Sabathier-Devals, G. Carlot, P. Matheron, X. Iltis, U. Pasquet, C. Valot, C. Delafoy, R. Largenton, Thermodynamics of chromium in UO_2 fuel: A solubility model, Journal of Nuclear Materials 447 (2014) 63–72. https://doi.org/10.1016/j.jnucmat.2013.12.021

[17] E. Gasnier, I. Bardez-Giboire, V. Montouillout, N. Pellerin, M. Allix, N. Massoni, S. Ory, M. Cabie, S. Poisonnet, D. Massiot, Homogeneity of Peraluminous SiO_2-B_2O_3-Al_2O_3-Na_2O-CaO-Nd_2O_3 Glasses: Effect of Neodymium Content, Journal of Non-Crystalline Solids 405 (2014) 55-62. https://doi.org/10.1016/j.jnoncrysol.2014.08.032

[18] V. Piovesan, Relations Composition-Structure-Propriétés des Verres Peralumineux pour le Conditionnement des Déchets Nucléaires, Thèse Université d'Orléans (2016). tel-01581258, version 1

[19] E. Hansen, D. Perret, I. Bardez-Giboire, S. Mure, C. Rapin, Structural and rheological analysis of nickel enriched peraluminous glasses, Journal of Non-Crystalline Solids: X (2021). https://doi.org/10.1016/j.nocx.2021.100069

[20] H. Khedim, R. Podor, P-J. Panteix, C. Rapin, M. Vilasi, Solubility of chromium oxide in binary soda-silicate melts, Journal of Non-Crystalline Solids 356 (2010) 2734-2741. https://doi.org/10.1016/j.jnoncrysol.2010.09.045

[21] J. Zhang, Z. Jiang, D. Jin, X. Liu, Preparation of nano-$Cr_{2-x}Al_xO_3$ (x=0–1) solid solution powders by using citrate-dispersant method, Materials Science and Engineering B 172 (2010) 33–36. https://doi.org/10.1016/j.mseb.2010.04.011

[22] A. Ramesh Babu, S. Yusub, P. M. Vinaya Teja, P. Srinivasa, V. Aruna, D. Krishna Rao, Effect of Cr_2O_3 on the structural optical and dielectric studies of LiF-SrO-B_2O_3 glasses, Journal of Non-Crystalline Solids 520 (2019) 119428. https://doi.org/10.1016/j.jnoncrysol.2019.05.004

[23]G. Calas, O. Majérus, L. Galoisy, L. Cormier, Crystal field spectroscopy of Cr^{3+} in glasses : Compositional dependence and thermal site expansion, Chemical Geology 229 (2006) 218-226. https://doi.org/10.1016/j.chemgeo.2006.01.021

[24] F. A. Moustafa, A. M. Fayad, F.M. Ezz-Eldin, I. El-Kashif, Effect of gamma irradiation on ultraviolet, visible and infrared studies of NiO, Cr_2O_3 and Fe_2O_3-doped alkali borate glasses, Journal of Non-Crystalline Solids 376 (2013) 18-25. https://doi.org/10.1016/j.jnoncrysol.2013.04.052

[25]A. Terczynska-Madej, K. Cholewa-Kowalska, M. Lacska, Coordination and valence state of transition metal ions in alkali-borate glasses, Optical Materials 33 (2011) 1984-1988. https://doi.org/10.1016/j.optmat.2011.03.046

[26] S. R. Ramanan, D. Ganguli, Spectroscopic studies of Cr-doped silica gels, Journal of Non-Crystalline Solids 212 (1997) 299-302. https://doi.org/10.1016/S0022-3093(97)00106-3

[27] E. Hansen, D. Perret, I. Bardez-Giboire, S. Diliberto, C. Rapin, Iron enriched peraluminous glasses: incorporation limit and effect of iron on glass transition temperature and viscosity, submitted for publication

[28] E. Schmucker, C. Petitjean, P-J. Panteix, L. Martinelli, S. Ben Lagha, M. Vilasi, Correlation between chromium physicochemical properties in silicate melts and the corrosion behavior of chromia-forming alloy, Journal of Nuclear Materials 510 (2018) 100-118. https://doi.org/10.1016/j.jnucmat.2018.07.059

[29] T. Murata, M. Torisaka, H. Takebe, K. Morinaga, Compositional dependence of the valency state of Cr ions in oxide glasses, Journal of Non-Crystalline Solids 220 (1997) 139-146. https://doi.org/10.1016/S0022-3093(97)00264-0

[30] Y. D. Yang, I. D. Sommerville, A. McLean, Some fundamental considerations pertaining to oxide melt interactions and their influence on steel quality, Trans. Indian Inst. Met., vol.59, No. 5, 2006.

[31] J. A. Duffy, Polarisability and polarising power of rare earth ions in glass: an optical basicity assessment, Physics and Chemistry of Glasses, Volume 46, Number 1 (2005) 1-6.

[32] T. Honma, Y. Benino, T. Fujiwara, T. Komatsu, R. Sato, V. Dimitrov, Electronic polarizability, optical basicity and interaction parameter of La_2O_3 and related glasses, Journal of Applied Physics 91 (2002) 2942. https://doi.org/10.1063/1.1436292

[33] J. B. Pedley, E. M. Marshall, J. Phys. Chem. Ref. Data, 12 (1984) 967. https://doi.org/10.1063/1.555698

[34] B. Cochain, Cinétique et Mécanismes d'Oxydoréduction dans les Silicates Fondus, Thèse Université Pierre et Marie Curie, Soutenue le 10/12/2009. https://hal-insu.archives-ouvertes.fr/tel-00813321

Appendix

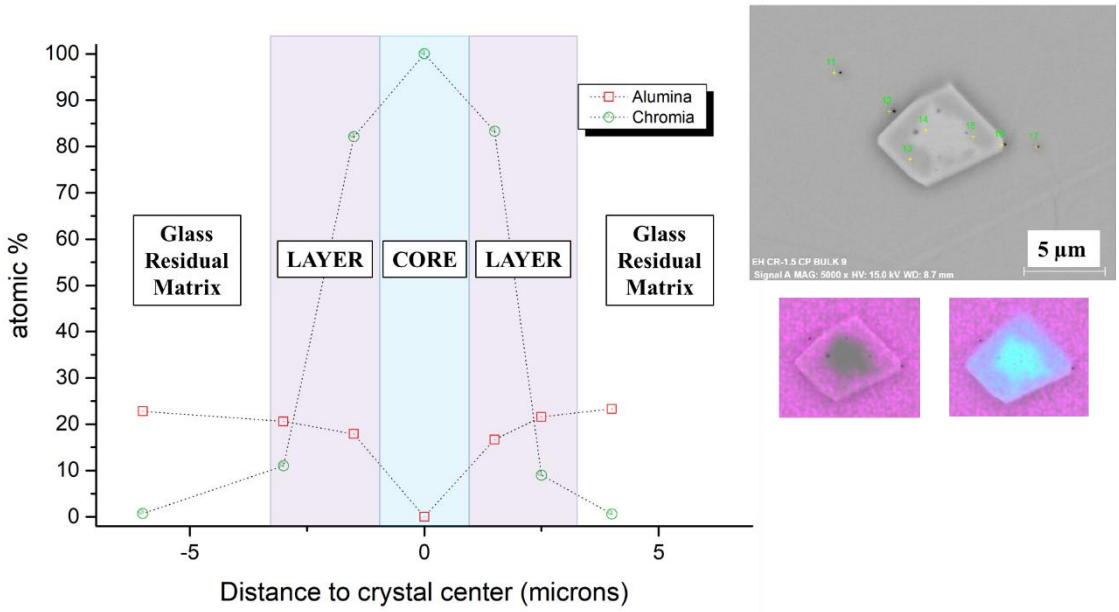

Figure 10: Composition of a crystal of the EH Cr-1.5 CP glass

Table 6: Composition of the crystal in the EH Cr-1.5 CP glass

Distance to center	6	3	1.5	0	1.5	2.5	4
Al_2O_3	22.8	20.6	17.9	0	16.7	21.6	23.3
Cr_2O_3	0.7	11.0	82.1	100	83.3	9.0	0.6
SiO_2	33.5	27.2				28.9	34.3
Na_2O	2.2	3.8				1.8	2.3
CaO	4.0	35.5				3.9	3.8
La_2O_3	36.7	1.5				34.9	35.7

*Table 7: Optical basicity table of the glass components in terms of oxides: * from Yang et al. [30], ** from Duffy [31], *** from Honma et al. [32]*

Oxide	Λ (optical basicity derived from Pauling)	Λ (optical basicity derived from average electron)
SiO_2	0.48*	0.47*
CaO	1 (reference)*	1 (reference)*
Li_2O	1.07*	1.05*
La_2O_3	1.18**	1.07***
Al_2O_3	0.61*	0.68*
B_2O_3	0.42*	0.42*
Na_2O	1.15*	1.1*
Cr_2O_3	***0.55****	***0.69****

Table 8: Basicity of the glasses calculated using the Pauling and Average electron method factors for oxides

Glass (Cr_2O_3 wt. %)	0 (base glass)	0.25	0.50	0.75	1.50
Basicity (Pauling)	0.582	0.582	0.582	0.582	0.582
Basicity (average electron)	0.583	0.583	0.584	0.584	0.584

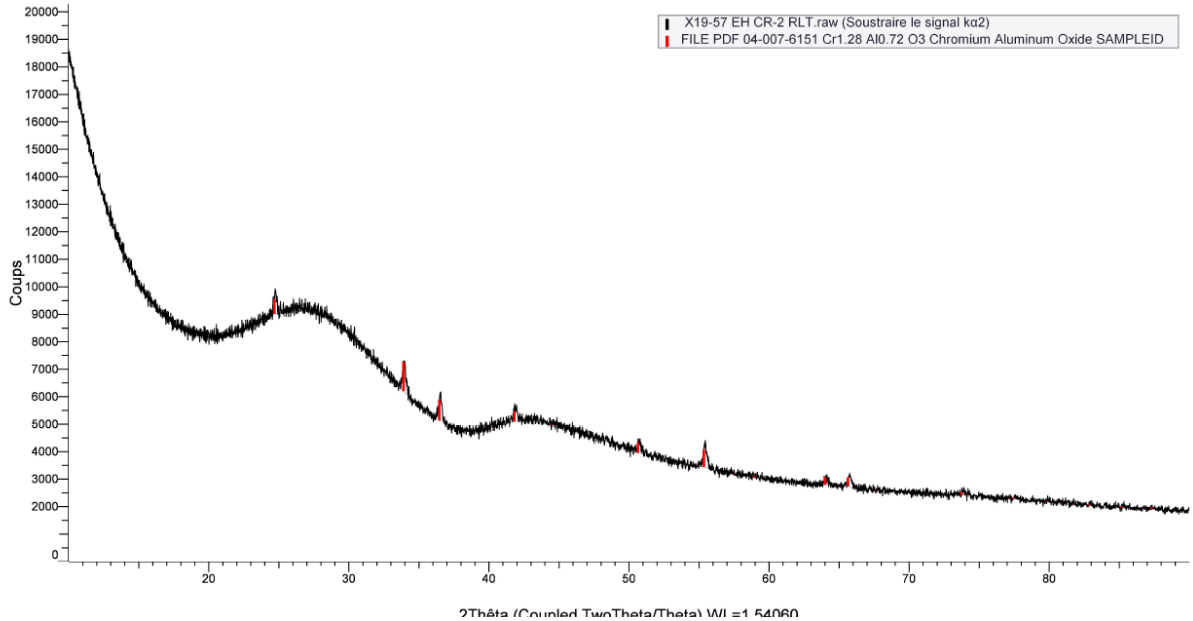

Figure 11: XRD diffractogram of the EH Cr-2 slowly cooled glass with the $Cr_{2-x}Al_xO_3$ phase